Toward ab Initio Intramolecular Dynamics

ROBERT E. WYATT*

Department of Chemistry and Biochemistry, University of Texas, Austin, Texas 78712

CHRISTOPHE IUNG AND CLAUDE LEFORESTIER

Laboratoire de Chimie Théorique, URA 506, Université de Paris-Sud, 91405 Orsay, France

Received December 12, 1994

Introduction

One of the central goals of chemical physics is to understand the nature of *intramolecular energy flow*.[1] It was emphasized[2] in 1982 that "intramolecular vibrational randomization processes (IVR)...have traditionally ranked high among the prime intellectual issues of chemical kinetics". The focus in studies of IVR involves answering questions such as the following: Starting from a well-defined initial excitation, where does the energy go? How long does it take to get there? To what extent is this flow state or mode specific? What is the detailed mechanism leading to the flow? What features of the energy surface are most important in determining the time scales and destination for the energy lost from the initial "hot spot"? How do spectral *features* measured in the frequency domain relate to *events* occurring in the time domain? What is the nature of the *dynamics that is induced in the background modes* when they acquire energy from the hot spot? During the past decade, considerable progress toward answering questions of this type has been made from both the experimental and theoretical directions.

Understanding intramolecular dynamics requires more than just applying simplistic but frequently useful ideas, such as the Fermi golden rule (FGR). Among other things, the FGR states that the rate of energy transfer out of the initial state should be proportional to the total density of states. The implication is that an $n = 2$ overtone, because it is embedded in a region of higher state density, should relax much faster than the $n = 1$ state. This is certainly correct in some cases. However, recent experimental results[1a] on the lifetimes of acetylenic CH stretch states in a series of molecules showed some surprising features. For example, in $(CH_3)_3SiCCH$, the CH lifetime for $n = 2$ is a factor of 2 *longer* than for $n = 1$, even though the density of states *increases* by a factor of 3000. Informative quantum mechanical calculations[3] have shown that a subset of coupled states in the first few tiers of background states coupled to the initial CH stretch controls the dynamics; the total state density does not play a significant role. This example and others mentioned later point to the need for quantum dynamical calculations to assist with the interpretation and correlation of experimental data. In addition, *dynamical calculations of this type can provide insights that would be impossible to glean from limited sets of experimental data.*

In this Account, we will discuss theoretical and computational developments in intramolecular dynamics and vibrational spectroscopy that have occurred since the early 1980s. In 1982, the theoretical situation was summarized,[2] "First principles prediction of the rates...is still well beyond the abilities of theory". However, because of a number of theoretical and computational developments, we believe that this situation has changed, at least for some interesting molecules. We will focus upon recently developed computational methods *that can be applied to multimode molecules described by accurate anharmonic force fields.* These methods have resulted in the most detailed studies yet to be reported on the spectra and dynamics of moderate-sized molecules. Because of the very large number of available quantum states, frequently $>10^6$, a number of new methods were developed, tested, and then incorporated into the production codes.

Through the use of these computational techniques, we will then present selected results on the overtone spectra and dynamics for 21-mode planar benzene. We will focus on the CH overtone dynamics because CH stretches are usually considered as local modes that are relatively decoupled from the other modes of the molecule. Consequently, one can expect that a molecule whose CH stretch is initially excited will exhibit interesting dynamical behavior that is not governed by purely statistical arguments. We have analyzed, in the past, molecules including CD_3H[4] and C_6H_6.[5] In these systems, the CH stretch is significantly coupled to the CH bend or wag adjacent to it. These closely linked modes are merged together and called the CH *chromophore.* Previous studies[6] have shown the crucial role played by Fermi resonance between the $|nv_{CH}\rangle$ and $|(n-1)v_{CH} + 2v_{CH(\text{wag or bend})}\rangle$ states. Conse-

Robert E. Wyatt obtained his Ph.D. in 1965 from The Johns Hopkins University. Following two years of postdoctoral research in England and at Harvard, he joined the faculty at the University of Texas at Austin.

Christophe Iung obtained his Ph.D. in 1990 from the Université de Paris at Orsay. From 1990 until 1995, he was on the faculty at Orsay.

Claude Leforestier obtained his Ph.D. in 1980 from the Université de Paris at Orsay. From 1981 until 1987, he was a research scientist at the CNRS at Orsay. From 1987 until 1995, he was on the faculty at Orsay.

(1) For reviews, see: (a) Lehman, K. K.; Scoles, G.; Pate, B. H. *Annu. Rev. Phys. Chem.* **1994,** *45,* 241. (b) Uzer, T. *Phys. Rep.* **1991,** *199,* 73.
(2) Smalley, R. E. *J. Phys. Chem.* **1982,** *86,* 3504.
(3) Stuchebrukhov, A. A.; Marcus, R. A. *J. Chem. Phys.* **1993,** *98,* 6044. Stuchebrukhov, A. A.; Mehta, A.; Marcus, R. A. *J. Phys. Chem.* **1993,** *97,* 12491.
(4) Iung, C.; Leforestier, C. *Comput. Phys. Commun.* **1991,** *63,* 135. Iung, C.; Leforestier, C. *J. Chem. Phys.* **1992,** *97,* 248.
(5) Wyatt, R. E.; Iung, C.; Leforestier, C. *J. Chem. Phys.* **1992,** *97,* 3458.
(6) Dübal, H. R.; Quack, M. *J. Chem. Phys.* **1984,** *81,* 3779. Lewerenz, M.; Quack, M. *J. Chem. Phys.* **1988,** *88,* 5408.

0001-4842/95/0128-0423$09.00/0

quently, the energy initially deposited in the CH stretch transfers quickly to the CH wag or bend. After this initial step, the energy can return to the CH stretch or go to the other vibrational modes of the molecule. In the CD_3H molecule, most of the energy in the CH chromophore remains there, even when the excitation energy is very high (16 000 cm^{-1}). By contrast, in the benzene molecule, the 19 nonchromophore modes, called *bath modes*, play an active role, even for the second CH overtone ($|3\nu_{CH}\rangle$, whose energy is about 8700 cm^{-1}).

For the studies described later, we will focus on the vibrational spectrum and will neglect vibration–rotation coupling. It is assumed that the total Hamiltonian operator H can be split into a zero-order Hamiltonian H^0 and a coupling operator W:

$$H = H^0 + W = \sum_{i=1}^{N_m} h_i^0 + W \qquad (1)$$

where N_m is the number of vibrational modes considered. The zero-order Hamiltonian will be written as the sum of zero-order Hamiltonians, h_i^0, each referring to one particular mode i. In these studies, the initially excited CH stretch will be described by a Morse oscillator Hamiltonian (local mode). By contrast, the other modes are normal modes described by harmonic oscillator Hamiltonians. The eigenstates of a given Hamiltonian h_i^0 are noted $|v_i\rangle^0$. The primary zero-order basis set, B, used in these calculations then consists of the direct product of the single-mode basis sets: $B = \{|v^{(1)}, ..., v^{(N_m)}\rangle^0, v^{(i)} \in [0, v^i_{max}]\}$. By contrast, the coupling operator, W, contains all of the vibrational coupling terms between the modes. It is generally estimated by ab initio quantum chemistry calculations and is expressed in terms of a Taylor series expansion in terms of displacements about the equilibrium molecular geometry.

Given this vibrational Hamiltonian, our goal is to investigate the vibrational spectrum and the time-dependent energy flow through an initially vibrationally excited molecule. From a quantum mechanical viewpoint, the *spectral calculation* involves solving the time-independent Schrodinger equation:

$$H|\Psi_\alpha\rangle = E_\alpha|\Psi_\alpha\rangle \qquad (2)$$

where the eigenstates $|\Psi_\alpha\rangle$ are expressed in terms of states in the zero-order basis set. Of course, the eigenvalues, E_α, are required in order to plot the vibrational spectrum. By contrast, analysis of the *energy flow* through the molecule requires the solution to the time-dependent Schrodinger equation

$$H|\psi(t)\rangle = i\hbar\frac{\partial|\psi(t)\rangle}{\partial t} \quad \text{with} \quad |\psi(t=0)\rangle = |i\rangle^0 \qquad (3)$$

The time-dependent wave function that satisfies this equation can be written in terms of the time evolution operator (propagator), $U(t)$:

$$U(t)|i\rangle^0 = |\psi(t)\rangle \quad \text{where} \quad U(t) = \exp(-iHt/\hbar) \qquad (4)$$

where $|i\rangle^0$ represents the initial state of the excited molecule. This can be, for instance, the $|3\nu_{CH}\rangle^0$ state, i.e., 3 quanta of vibrational energy in one local CH stretch. Calculation and analysis of the evolving wavepacket $|\psi(t)\rangle$ permits one to study and analyze IVR by quantum mechanical methods.

The Large Quantum Dynamical Problem

The first problem faced in large-scale quantum mechanical studies concerns the huge dimension of the primitive basis set, B. For instance, even if we limit our investigation to the 21 in-plane modes of benzene, the study of the second CH overtone, $|3\nu_{CH}\rangle^0$, requires that we set all of the parameters v^i_{max} to at least 4. This results in a primitive basis set containing more than 4×10^{14} states! A smaller molecule, such as CF_3H, requires primitive basis sets containing millions of states. This dimension is so large that direct dynamical studies are precluded. We have shown[4] that no simplistic energy criteria can be used in order to reduce this dimension. Fortunately, all of these states are not involved in the CH overtone dynamics. Consequently, we will extract from the primitive space (using perturbation theory) a subspace, called the *active space*, containing all of the zero-order states which are "actively involved" in the CH overtone dynamics. This subspace, containing from 5000 to 20 000 basis functions, may still be quite large.

Construction of the Active Space

How can we extract several thousand "active states" from the huge primitive space, which contains millions or billions of zero-order states? The first method that we will mention for constructing the active space uses artificial intelligence (AI) tree-pruning algorithms. A number of studies have employed various AI methods.[7] The key steps are *search, evaluate, and select*. When the desired number of states has been selected, the search terminates and in a sense we have pruned the search tree by not exploring and generating the rest of the tree. Along with the initial state, this set of selected states now constitutes the active space. There are two aspects to the selection process, one concerning tactics (the *local search*), the other concerning strategy (choosing *entire paths* through the state space). In many cases, entire paths are desired; the states lying along these paths form the active space. For the intramolecular dynamics problem, first-order perturbation theory is frequently used in the tactical search. One of the main drawbacks with the AI algorithm arises from the imposition of energy criteria to reduce the dimension of the active space. Computational studies have shown that this approximation can lead to erroneous results.[8] Consequently, other methods which are more flexible and do not use an arbitrary energy cutoff are desired for constructing the active space. For this reason, we will focus on the use of perturbation theory. In this approach, the full Hamiltonian, H, is subdivided into two operators (see eq 1): H^0, the zero-order Hamiltonian, and W, the coupling operator.

(7) Tietz, J. V.; Chu, S.-I. *Chem. Phys. Lett.* **1983**, *101*, 446. Chang, J.; Wyatt, R. E. *Chem. Phys. Lett.* **1985**, *121*, 307. Lederman, S. M.; Marcus, R. A. *J. Chem. Phys.* **1988**, *88*, 6312. Colbert, D. T.; Sibert, E. L., III. *J. Chem. Phys.* **1991**, *94*, 6519.

(8) Iung, C.; Leforestier, C.; Wyatt, R. E. *J. Chem. Phys.* **1993**, *98*, 6722.

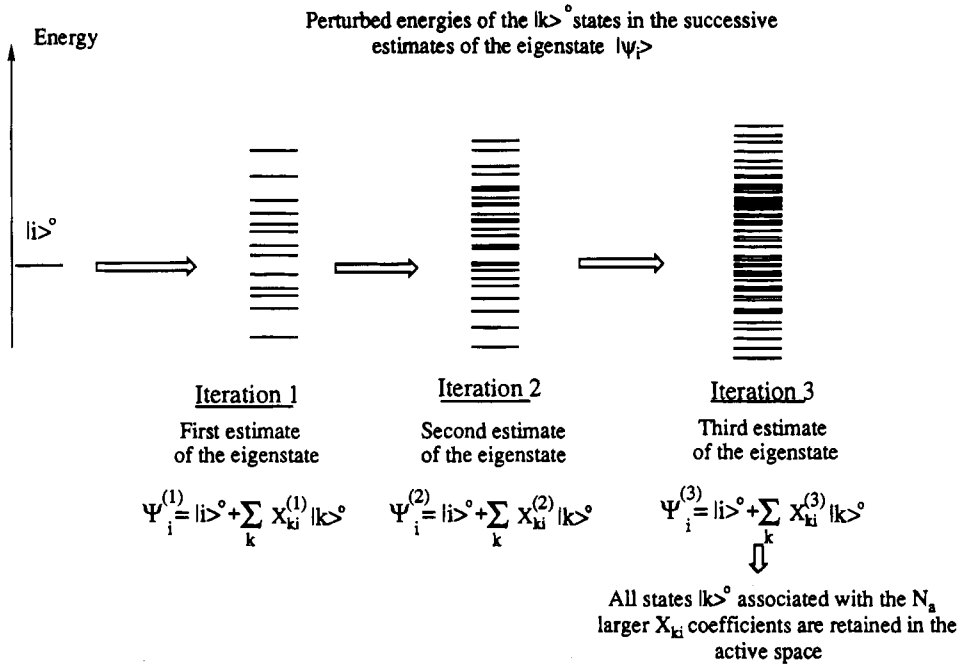

Figure 1. Wave operator sorting algorithm for building an active space. Basis states in the primitive space are included in the active space if the amplitude $X_{ki}^{(n)}$ is relatively large in magnitude. In this example, three iterations of the algorithm were performed, $n = 3$.

In the perturbative approach, we will define the *wave operator* Ω as the operator which maps zero-order vectors into exact eigenvectors,[9] i.e., $\Omega|i\rangle^0 = |\Psi_i\rangle$. The aim of the Bloch formalism is to construct a perturbative expansion for the wave operator. We will first introduce the *transition operator*[10] X and write Ω as $\Omega = P^0 + X$, where P^0 projects onto the initial state and where the operator X links $|i\rangle^0$ to the other states in the primitive space. In the applications presented below, a treatment called the *recursive distorted wave approximation*[11] (RDWA) has been used to generate the X-operator matrix elements. At each iteration step, this procedure involves the evaluation of the kth order operator $X^{(k)}$ and the effective Hamiltonian $H^{(k+1)}$, which is then used to calculate $X^{(k+1)}$, and so on.

The main steps in the wave operator algorithm for constructing an active space from the large primitive basis sets are illustrated in Figure 1. Assume now that N iterations of the transition operator have been performed. As a result, a large number of nonzero matrix elements X_{ki} have been generated. (As indicated above, the matrix element X_{ki} measures the strength of the linkage between the initial state and basis function $|k\rangle^0$ in the primitive space.) The basis functions $|k\rangle^0$ are then reordered such that those having the largest magnitude of X_{ki} are up near the top of the list. Then, the top N_a basis functions are selected for inclusion in the active space; the remaining $N_a + 1, \ldots, N$ basis functions are discarded. Clearly, N_a is the dimension of this active space.

One feature that the wave operator sorting algorithm shares with the AI tree pruning algorithm is that successive tiers of states are generated. However, the wave operator algorithm does not use an energy window during the selection process. In practice, some states with large detunings from the initial state are selected for inclusion in the active space by the wave operator. We have recently shown that *the wave operator sorting algorithm is more efficient at building the active space than the more traditional intelligence AI tree-pruning procedure.*[8]

Spectral Calculations in the Active Space

The dimension of the active space (frequently from 5000 to 20 000 states) prevents standard direct diagonalization of the Hamiltonian matrix. Actually, not all of the information resulting from a matrix diagonalization is needed. In fact, we are attempting to compute the *line shape function* associated with transitions from the ground state, $|\Psi_g\rangle$. The line shape function is defined by

$$S(E) = \sum_\alpha |\langle\Psi_g|\mu|\Psi_\alpha\rangle|^2 L(E - E_\alpha) \qquad (5)$$

where $|\Psi_\alpha\rangle$ is the eigenfunction corresponding to the eigenvalue E_α. The quantity $\langle\Psi_g|\mu|\Psi_\alpha\rangle$ is the *dipole matrix element* linking the ground state with eigenstate $|\Psi_\alpha\rangle$; the absolute square of this quantity is the line intensity. The line shape function for each spectral line is frequently assumed to be a normalized *Lorentzian* function. In the case of CH overtones, we can assume that the major contribution to the dipole transition moment arises from the local CH mode. As a result, the absorption spectrum is proportional to the *residue spectrum*, $S'(E)$, given by

$$S'(E) = \sum_\alpha |^0\langle n\nu_{CH}|\Psi_\alpha\rangle|^2 L(E - E_\alpha) \qquad (6)$$

in which $|n\nu_{CH}\rangle^0$ is the (local mode) CH overtone state and the quantities $|^0\langle n\nu_{CH}|\Psi_\alpha\rangle|^2$ are called the *residues*. The residue can be viewed as the probability of finding the spectrally active "bright state" in the eigenstate $|\Psi_\alpha\rangle$. Figure 2 illustrates the notion of a residue spectrum.

(9) Bloch, C. *Nucl. Phys.* **1958**, *6*, 329.
(10) Lindgren, L. *J. Phys. B* **1974**, *7*, 2441.
(11) Jolicard, G. *Chem. Phys.* **1988**, *127*, 31.

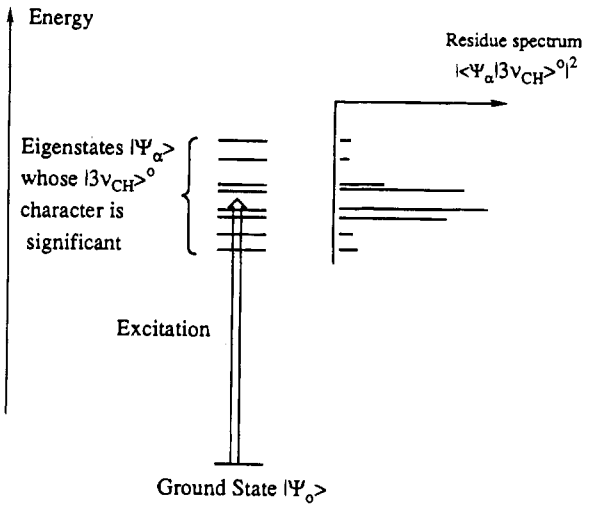

Figure 2. Residue spectrum from the ground state to a set of eigenstates whose bright state $|n\nu_{CH}\rangle^0$ character is significant. Each residue gives the probability of finding the bright state in an eigenstate.

The recursive residue generation method[12] (RRGM) will be used in order to calculate the residue spectrum. Given the Hamiltonian and the initial state $|n\nu_{CH}\rangle^0$, the RRGM focuses upon computation of the residues and eigenvalues which are required to compute the spectrum, *without computing the eigenvectors*. The core of the RRGM utilizes the Lanczos algorithm[13] for transforming a matrix into a smaller tridiagonal form. The idea is, in stepwise fashion, to develop an $M \times M$ tridiagonal matrix **T**, in which M is frequently much smaller than the dimension of the active space, N. After performing M Lanczos recursion steps, we will have computed the diagonal and off-diagonal elements in the tridiagonal matrix **T**. From **T**, we can then quickly compute M eigenvalues and residues. This, in turn, permits an M-term approximation to the residue spectrum. Of course, it is necessary to verify convergence by examining the spectra for several values of M.

IVR Calculations in the Active Space

We will again assume that the system is initially described by the zero-order state $|i\rangle^0$, which might be a CH overtone state $|n\nu_{CH}\rangle^0$. In order to compute the time-evolving state, $|\psi(t)\rangle$, we use an expansion of the time evolution operator (see eq 4), $U(\Delta t)$, in terms of Chebyshev polynomials[14] (where Δt might be, for instance, 50 fs). Consequently, $|\psi(t+\Delta t)\rangle$ can be generated by applying the evolution operator, $U(\Delta t)$, onto the state vector $|\psi(t)\rangle$. This efficient (but time-consuming) approach gives an expansion of the time-evolving wave packet in terms of the zero-order states belonging to the active space.

Spectroscopy and Dynamics for C_6H_6

A demanding application of the ideas discussed above concerns the overtone spectroscopy and dynamics of energy flow in benzene. This section will emphasize our recent quantum mechanical studies of 21-mode planar benzene.[15] We will begin by reviewing some of the previous experimental and theoretical studies. In important experiments conducted around 1980, Berry and co-workers recorded overtone spectra of room temperature gas phase benzene.[16] They reported broad absorption features; for $n = 3$, the roughly 100 cm^{-1} FWHM asymmetric absorption feature had a broad shoulder on the red side of the main feature. The experimental situation advanced significantly when Page et al.[17] reported results for the $n = 1$, 2, and 3 CH excitations using the supersonic molecular beam technique. Recently, Scotoni et al.[18] reported additional spectra for both the $n = 3$ and 4 overtones. Under their beam conditions, the $n = 3$ spectrum also showed a main peak at 8827 cm^{-1}, but with at least 5 less prominent bands on the "red" side of the main peak.

Using both classical and quantum mechanical models, Sibert *et al.*[19] made detailed comparisons with the experimental results of Berry et al. Their model assumed *only kinetic energy coupling* in curvilinear coordinates, the most important of which was between the CH stretch and the contiguous CCH in-plane wag. The spectra predicted by this model appeared to be in good agreement with the experimental data that was available in 1982. In addition to our recent studies, Zhang and Marcus[20] have computed spectra and survival probabilities. An extensive series of classical trajectory studies on overtone relaxation in benzene have also been reported.[21] We will briefly return to the classical results later in this Account.

Since 1980, considerable computational effort has been devoted to the determination of an accurate force field for benzene. Recently, after years of detailed experimental and theoretical studies, Goodman and co-workers[22] reported a benchmark *harmonic force field* by combining all currently available experimental information with theoretical calculations. The first ab initio force field to incorporate both harmonic and anharmonic force constants (some cubic force constants) was reported by Pulay et al.[23] in 1981. The computed harmonic force constants, as expected, were larger than the empirical values, so a scaled quadratic force field was developed. The more recent 1992 Maslen et al.[24] force field was computed by evaluating *analytic derivatives* through quartic terms at the SCF

(12) Nauts, A.; Wyatt, R. E. *Phys. Rev. Lett.* **1983**, *81*, 2238. Wyatt, R. E. *Adv. Chem. Phys.* **1989**, *73*, 231.
(13) Lanczos, C. *J. Res. Natl. Bur. Stand.* **1950**, *45*, 58.
(14) Tal-Ezer, H.; Kosloff, R. *J. Chem. Phys.* **1984**, *81*, 3967.
(15) (a) Wyatt, R. E.; Iung, C.; Leforestier, C. *J. Chem. Phys.* **1992**, *97*, 3458, (b) 3477. (c) Wyatt, R. E.; Iung, C. *J. Chem. Phys.* **1993**, *98*, 3577, (d) 5191, (e) 6758. (f) Iung, C.; Wyatt, R. E. *J. Chem. Phys.* **1993**, *99*, 2261.
(16) Reddy, R. V.; Heller, D. F.; Berry, M. J. *J. Chem. Phys.* **1982**, *76*, 2814.
(17) Page, R. H.; Shen, Y. R.; Lee, Y. T. *J. Chem. Phys.* **1988**, *88*, 4621, 5362.
(18) Scotoni, M.; Boschetti, A.; Oberhofer, N.; Bassi, D. *J. Chem. Phys.* **1991**, *94*, 971. Scotoni, M.; Leonardi, C.; Bassi, D. *J. Chem. Phys.* **1991**, *95*, 8655.
(19) Sibert, E. L.; Reinhardt, W. P.; Hynes, J. T. *J. Chem. Phys.* **1984**, *81*, 1115, 1135.
(20) Zhang, Y.; Klippenstein, S. J.; Marcus, R. A. *J. Chem. Phys.* **1984**, *94*, 7319. Zhang, Y.; Marcus, R. A. *J. Chem. Phys.* **1992**, *96*, 6065, 5283.
(21) Lu, D. H.; Hase, W. L. *J. Phys. Chem.* **1988**, *92*, 3217; *J. Chem. Phys.* **1989**, *91*, 7490. Clarke, D. L.; Collins, M. A. *J. Chem. Phys.* **1987**, *86*, 6871; *87*, 5912. Guan, Y.; Thompson, D. L. *J. Chem. Phys.* **1988**, *88*, 2355. Gomez-Llorente, J. M.; Hahn, O.; Taylor, H. S. *J. Chem. Phys.* **1990**, *92*, 2762. Garcia-Ayllon, A.; Santamaria, J.; Ezra, G. S. *J. Chem. Phys.* **1988**, *89*, 801.
(22) Goodman, L.; Ozkabak, A. G.; Thakur, S. N. *J. Phys. Chem.* **1991**, *95*, 9044.
(23) Pulay, P.; Fogarasi, G.; Boggs, J. E. *J. Chem. Phys.* **1981**, *74*, 3999.
(24) Maslen, P. E.; Handy, N. C.; Amos, R. D.; Jayatilaka, D. *J. Chem. Phys.* **1992**, *97*, 4233.

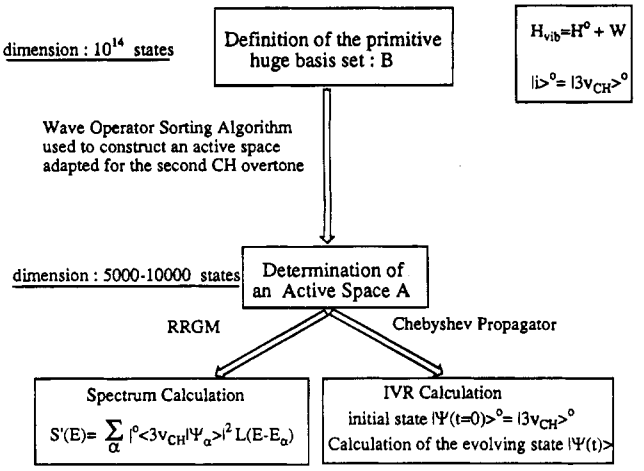

Figure 3. Methodology followed in order to study the second CH overtone, $|3v_{CH}\rangle^0$. The RRGM is used to compute spectra and survival probabilities, and the Chebyshev expansion of the time evolution operator is used to compute the detailed wave packet evolution.

level. Following a procedure similar to that of Pulay et al.,[23] we have developed a new ab initio force field for describing the CH chromophore and used the Maslen et al. force field[15e] for the other couplings. The result is a quartic force field for all couplings between bath modes or between bath modes and chromophore modes, while an eighth-order expansion has been used in order to reproduce accurately the stretch-wag couplings within the chromophore.

Overtone Spectrum and Survival Probability for C_6H_6

Figure 3 summarizes the computational strategy that we have followed in order to study either the overtone spectrum or the flow of vibrational energy in benzene. The computed overtone spectrum is shown in Figure 4a (solid curve), and the survival probability is shown in Figure 4b. The survival exhibits rapid initial falloff, declining below 0.025 by $t = 0.24$ ps. (As a calibration, the harmonic period for a CH vibration is about 0.01 ps.) After this time, the survival shows a series of low amplitude recurrence oscillations extending to $t = 1.2$ ps and beyond. This figure shows that the dephasing time for the initial state is about 0.2 ps. If the survival amplitude is first multiplied by a cutoff function which decreases rapidly after the dephasing time and the product is then Fourier transformed back to the frequency domain, we obtain the broad envelope of the spectrum shown in Figure 4a.

We mentioned earlier that two experimental groups[17,18] have recently measured CH(n=3) overtone spectra in benzene. These experimental spectra were reconstructed with a set of Lorentzian functions, see Figure 5a. The survival computed from the Fourier transform of the Page et al. experimental spectrum is displayed in Figure 5b. We note rapid falloff of $S(t)$ by $t = 0.2$ ps, and recurrence phenomena at later times. The computed spectrum and survival can be compared with the experimental results. The computed spectra in Figure 4a have a slightly higher intensity over the interval -50 to $+70$ cm^{-1} when compared with the experimental spectrum of Scotoni et al., but there is at least qualitative agreement with

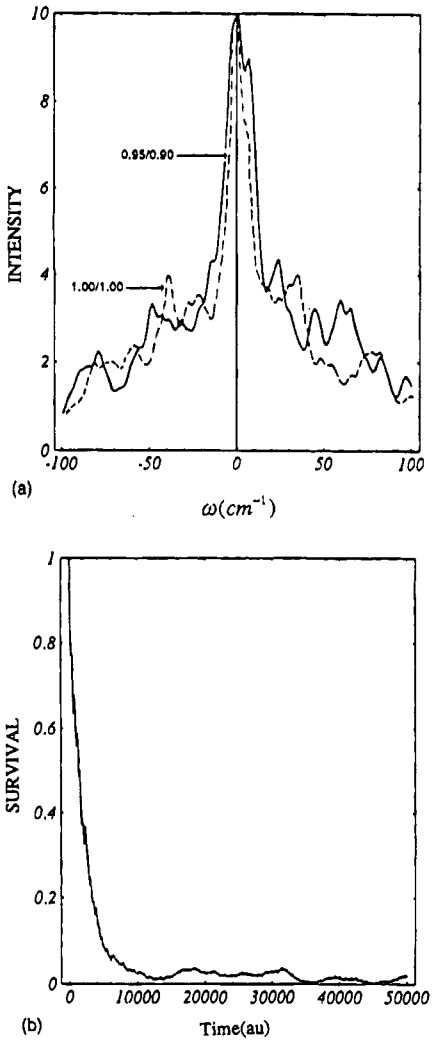

Figure 4. (a) Computed CH(n=3) overtone spectrum for benzene and (b) survival probability. In panel a, the peak intensity has been scaled to the value 10. Also in panel a, spectra are shown for two values of the anharmonic scaling parameters: continuous curve, $a = 0.95$, $b = 0.90$ (scaled potential); dashed curve, $a = b = 1.0$ (unscaled potential). These parameters multiply the CH–ring and ring–ring anharmonic coupling terms, respectively. The survival was computed using the scaled potential.

the results of Page et al. Compared with the experimental results, the survival shown in Figure 4b shows more rapid falloff at short times, $t < 0.12$ ps. This is expected, since the experimental spectra are available over a limited ($\sim$200 cm^{-1}) frequency window. After $t = 0.5$ ps, the computed survival shows a sequence of low amplitude recurrence oscillations; this amplitude agrees qualitatively with the experimental results.

We mentioned earlier that a number of classical trajectory studies have been reported for benzene.[21] Unfortunately, definitive comparisons cannot be made at this time between the quantum and the classical results, because different potential surfaces have been used. (Trajectory studies have not been reported on the relatively accurate ab initio force field[24] that we used in the quantum studies.) However, it is possible to make some qualitative comparisons. One important observation is that there is very good agreement between the short-time ($t < 0.15$ ps) values of the quantum and classical survival probabilities (the classical results of Lu and Hase[21] were used). This agreement is obtained when the trajectories are run

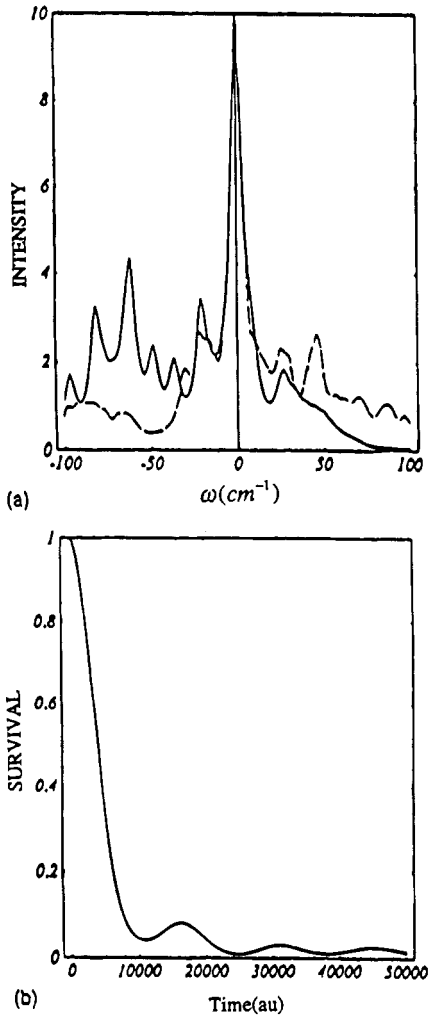

Figure 5. Reconstructions of the experimental $n = 3$ overtone spectra for benzene. (a) Spectra of Page et al.[17] (dashed curve) and Scotoni et al.[18] This experimental data extends to about +40 cm^{-1} from the central peak. In both spectra, the central peak occurs at 8827 cm^{-1}. (b) Survival probability computed from the spectrum of Page et al.[17]

with the energy equivalent of zero-point energy, but not if it is neglected. At longer times, the averaged classical survival does not show the detailed recurrence structure shown by the quantum calculations. However, definitive comparisons will have to wait for the completion of trajectory studies on the same potential that was used in the quantum studies.

Time-Dependent Study of Energy Flow in C_6H_6

In order to answer the basic questions concerning the nature of IVR that were posed in the opening paragraph of this Account, a time-dependent internal mode analysis must be performed.[15f] Using the Chebyshev expansion of the time propagator, we have calculated the time-evolving wave packet, $|\psi(t)\rangle$, for the system described by the initial state $|3\nu_{CH}\rangle^0$, i.e., 3 quanta of vibrational energy in one CH stretch with the other modes unexcited. This time-evolving wave packet was expressed in terms of zero-order basis functions that involve normal modes, i.e., delocalized vibrational modes. In order to analyze the energy flow in the molecule, the time dependence of the average energy in each of the local modes was computed. Local

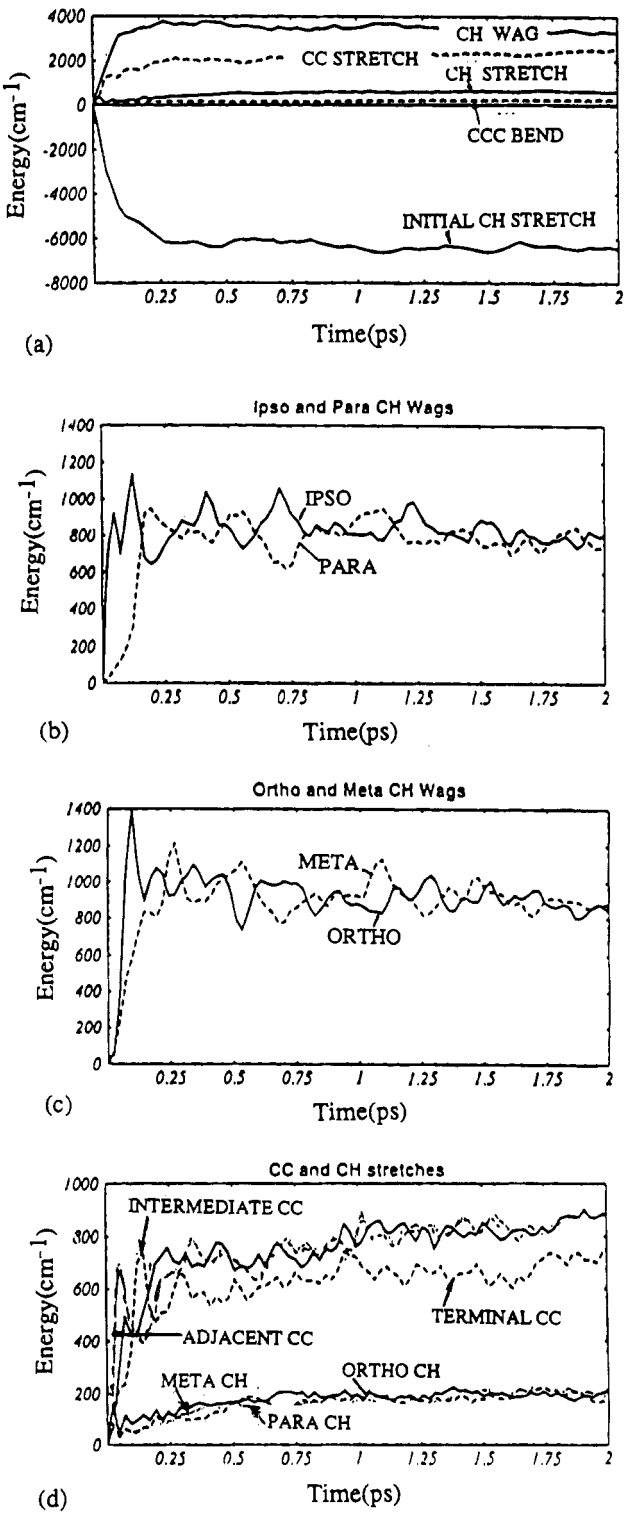

Figure 6. (a) Variation in average vibrational energy vs time for relaxation from the CH(n=3) overtone in benzene. The energy lost from the initially excited CH stretch and the energy gained for the other local modes are shown. Total energies are shown for six CH stretch, six CC stretch, six CCH wag, and three CCC bend modes. The energy growth for three types of local modes are shown; (b) ipso and para CCH wags; (c) two ortho and two meta wags; (d) pairs of adjacent, central, and terminal CC stretches. The energies in the pair of ortho and meta CH stretches are also shown, along with the energy of the para stretch.

mode Hamiltonians, $H_i^{(1)}$, for internal coordinate i, were defined in terms of the harmonic potential. However, when considering the energy of the initially excited CH oscillator, a Morse oscillator Hamiltonian

was used. The average energy for local mode i at time t is then the expectation value, $\langle E_i(t)\rangle = \langle\psi(t)|H_i^{(1)}|\psi(t)\rangle$.

Figure 6a shows the decline in energy of the initially excited CH stretch, along with the growth in energy of the initially unexcited CH stretches, CH wags, and CC stretches. This 2 ps time interval corresponds to about 200 CH or to about 80 CC or CH harmonic vibrational periods. At short times, the initially unexcited modes *simultaneously* gain energy, but the *rate of energy uptake* follows the ordering CH wags > CC stretches > CH stretches > CCC bends. The largest amount of energy goes into the six low-frequency CH wags (3200 cm^{-1} at 2 ps), followed by the six CC stretches (2500 cm^{-1} at 2 ps). In addition, about 600 cm^{-1} is acquired by the five initially unexcited CH stretches. We also note that the energy in the CH wags and the CC stretches reaches an approximate steady-state value after about 1.0 ps, while the energy of the unexcited CH stretches and the CCC bends continues to slowly increase.

Panels b–d of Figure 6 provide a more detailed view of the energy transfer and display the *complex dynamics induced in the background modes* when they are driven by the energy acquired from the relaxing CH oscillator. First, Figure 6b,c shows the energy in the four types of CH wag motion, while Figure 6d shows the energy in the three different types of CC stretches and the initially unexcited CH stretches. At short times, $t < 0.2$ ps, the energy goes first into the ipso CH wag, then into the adjacent CC stretches, then into both the central CC stretches and the ortho CH wags, then into both the terminal CC stretches and the meta CH wags, and finally into the para wag at about $t = 0.20$ ps. During the next 0.2 ps, part of the energy returns to the ipso CH wag. During the next 0.2 ps, the energies of the CH wags and the CC stretches approach their average steady-state values. *Then, for $t > 0.6$ ps, we note an important coherent oscillation involving wag (or CC) motion at opposite ends of the molecule: the wag (or CC stretch) energy oscillates between the ipso and para positions.* This internal clock continues to beat with a period of about 0.3 ps, which can be considered as the time required to go from the ipso to the para position and then to return to the ipso position. These oscillations represent a relatively long distance correlation between local modes at opposite ends of the molecule. Figure 6d also shows the time dependence of energy transfer into the five initially unexcited CH stretches. For $t < 2$ ps, these modes play a secondary role. Finally, we note that, at $t = 2$ ps, about 37% of the energy released from the initially excited CH stretch ends up in the CCH wag motions, 29% goes to the CC stretches, 7% goes to the initially unexcited CH stretches, and 3% goes to the CCC bends. About 24% of the energy still remains in the initially excited CH stretch. *On the time scale of several picoseconds, this partitioning of energy is not statistical.*

Outlook

Due to theoretical and computational developments during the past 12 years, it has become possible to start with accurate ab initio force field information and then perform large-scale quantum dynamical calculations on moderate-sized molecules of chemical interest.[25] We are approaching the era when ab initio quantum dynamical calculations on molecules or molecular fragments with 10–30 vibrational modes will become increasingly feasible. The resulting predictions of spectra and intramolecular energy flow will nicely complement experimental advances which are directed toward answering the same fundamental questions.

We wish to thank the National Science Foundation and the Robert Welch Foundation for supporting this research.

AR940089B

(25) For a more extensive review, see: Wyatt, R. E.; Iung, C. In *Dynamics of molecules and chemical reactions*; Wyatt, R. E., Zhang, J. H., Eds.; Marcel Dekker: New York, 1995.